Molecular Therapy
Oncolytics
Original Article

TRIM22 orchestrates the proliferation of GBMs and the benefits of TMZ by coordinating the modification and degradation of RIG-I

Xiaowei Fei,[1,3] Xiuquan Wu,[1,3] Ya-Nan Dou,[1,3] Kai Sun,[2] Qingdong Guo,[1] Lei Zhang,[1] Sanzhong Li,[1] Jialiang Wei,[1] Yu Huan,[1] Xin He,[1] and Zhou Fei[1]

[1]Department of Neurosurgery, Xijing Hospital, Air Force Military Medical University, Xi'an, Shaanxi 710032, China; [2]Department of Neurosurgery, Daping Hospital, Third Military Medical University, Chongqing 400042, China

Tripartite motif 22 (TRIM22) is an agonist of nuclear factor κB (NF-κB) that plays an important role in the proliferation and drug sensitivity of glioblastoma (GBM). However, the molecular mechanism underlying the protein network between TRIM22 and nuclear factor κB (NF-κB) in GBM remains unclear. Here, we found that knockout of *TRIM22* effectively inhibited tumor proliferation and increased the sensitivity of GBM cells to temozolomide (TMZ) *in vivo* and *in vitro*. Moreover, TRIM22 forms a complex with cytosolic purine 5-nucleotidase (NT5C2) in GBM and regulates the ubiquitination of retinoic acid-inducible gene-I (RIG-I). TRIM22 promotes the K63-linked ubiquitination of RIG-I, while NT5C2 is responsible for K48-linked ubiquitination. This regulation directly affects the RIG-I/NF-κB/cell division cycle and apoptosis regulator protein 1 (CCAR1) signaling axis. Ubiquitin modification inhibitor of RIG-I restores the inhibition of tumor growth induced by *TRIM22* knockout. The follow-up results showed that compared with patients with high TRIM22 expression, patients with low TRIM22 expression had a longer survival time and were more sensitive to treatment with TMZ. Our results revealed that the TRIM22-NT5C2 complex orchestrates the proliferation of GBM and benefits of TMZ through post-translational modification of RIG-I and the regulation of the RIG-I/NF-κB/CCAR1 pathway and is a promising target for single-pathway multi-target therapy.

INTRODUCTION

Glioma is the most common malignancy of the central nervous system, and patients with high-grade gliomas have a poor prognosis and short survival.[1] The use of temozolomide (TMZ) can significantly prolong the survival of patients with high-grade glioma, but drug resistance is increasingly becoming prevalent in patients with this disease.[2,3] As cancer treatment has entered the era of targeted molecular therapy,[4] many glioma-associated gene mutations, such as the 19q deletion, have been discovered in recent years.[5] The targeted therapies currently used for glioma include the epidermal growth factor receptor tyrosine kinase inhibitor gefitinib,[6] the vascular endothelial growth factor receptor inhibitor avastin,[7] and the anti-CD20 monoclonal antibody rituximab.[8] It is hoped that therapies targeting multiple signaling pathways or multiple targets in the same signaling pathway are more effective than therapies with single targets. Clinical trials for glioma investigational drugs, such as marimastat in combination with TMZ[9] and imatinib in combination with hydroxyurea,[10] have provided encouraging preliminary results.

Tripartite motif 22 (TRIM22), a member of the TRIM family, is involved in a variety of biological processes, such as cell proliferation,[11,12] differentiation,[12,13] carcinogenesis,[14] and apoptosis.[15] Owing to its conserved structural characteristics and E3 ubiquitin ligase activity,[16] it is used as a biomarker for targeted therapy in the study of many tumors. TRIM22 inhibits the progression of endometrial cancer through the NOD2/nuclear factor κB (NF-κB) signaling pathway and improves prognosis.[17] However, to date, only one report has revealed the role of TRIM22 in glioma, suggesting that TRIM22 activates NF-κB signaling in glioblastoma (GBM) by accelerating the degradation of IκBα.[18] The development of inhibitors targeting NF-κB has received attention from experts in glioma.[19] However, with the large number of negative effects caused by this inhibitor and the uncertain effectiveness of simultaneous treatment with this inhibitor on multiple targets, it is imperative to explore a targeted drug that can be used in combination with NF-κB inhibitors. However, the NF-κB pathway plays an "intersection" role in many signal transduction pathways. Its upstream region is affected by various molecules, and its downstream region can regulate gene transcription. Although it has been found that TRIM22 can affect the NF-κB pathway, the specific regulatory mechanism between TRIM22 and NF-κB is unknown.

Our studies are further exploring the potential role of TRIM22 in GBM and investigating the possible protein network mechanism

Received 26 October 2021; accepted 19 August 2022;
https://doi.org/10.1016/j.omto.2022.08.007.

[3]These authors contributed equally

Correspondence: Zhou Fei, Department of Neurosurgery, Xijing Hospital, Air Force Military Medical University, Xi'an, Shaanxi 710032, China.
E-mail: feizhou@fmmu.edu.cn

between TRIM22 and NF-κB, providing new clues for targeted combination therapies for GBM.

RESULTS

TRIM22 is highly expressed in gliomas and is positively correlated with tumor grade

To explore and validate the expression of TRIM22 in gliomas, we analyzed the GEPIA2 (Figure 1A) and Oncomine (Figure 1B) databases and found that TRIM22 was highly expressed in GBM compared with normal brain tissue. *TRIM22* has been reported as a target gene of TP53,[20] and the GEPIA2 database showed that *TP53* is the gene with the second-highest mutation rate in gliomas (Figure 1C). Therefore, we speculated that high TRIM22 expression plays an indispensable role in glioma. Immunohistochemical staining was performed to validate the results we obtained from the database analysis (Figure 1D). The results showed that TRIM22 was highly expressed in gliomas compared with normal brain tissue and was positively correlated with tumor grade (Figure 1E). In addition, we performed western blotting on four cell lines and nine fresh clinical GBM specimens. We found that TRIM22 was more highly expressed in U251MG cells than in U87MG, U118, and T98G cells and that TRIM22 was more highly expressed in grade IV gliomas than in gliomas of lower grades (Figure 1F).

To further explore the role of TRIM22 in GBM, we introduced U251MG cells intracranially into mice via stereotactic injection. The experimental group group 1 (G1, n = 11) was used as the control, while G2 (n = 11) was the TRIM22-knockdown group. Twenty-one days after surgery, we found that the fluorescence intensity reached a maximum at 8 min after intraperitoneal injection of fluorescein sodium salt and that the fluorescence intensity was significantly different between the G1 and G2 groups (Figures 1G and 1H). In addition, the mice in the G2 group had better survival than those in the G1 group (Figure 1I), but there was no apparent difference in body weight between the two groups (Figure 1J). These results preliminarily indicate that TRIM22 knockdown inhibits GBM cell proliferation *in vivo*.

In addition, we analyzed the survival of patients with glioma with different TRIM22 expression levels using the GSCA database. We found that the progression-free survival (PFS) and overall survival (OS) of patients with GBM were not related to the expression of TRIM22. However, patients with low-grade glioma (LGG) with low TRIM22 expression had better PFS (Figure 1K). These results were inconsistent with the results of our previous research since Ji et al.[18] also reported that TRIM22 is correlated with a poor survival rate in GBM. Combined with our experimental results, we speculate that the negative results may be due to the small number of patients in the GSCA database and that TRIM22 may correlate with poor survival rate in GBM. More samples and experiments are required to verify the relationship between TRIM22 expression and high-grade gliomas.

TRIM22 knockout significantly inhibited the proliferation of gliomas *in vivo* and *in vitro* and improved the benefits of TMZ

To investigate the effect of *TRIM22* knockout on glioma and its effect on TMZ efficacy, we cultured clinically derived cell lines P1, P2, and P3 and performed short tandem repeat (STR) identification and pathological diagnosis (Table S1) to confirm the origin of GBM. Using CRISPR-Cas9 technology (Figure S1A), we knocked out *TRIM22* in the U251MG, P1, P2, and P3 cell lines. We found that both TMZ treatment and knockout of *TRIM22* significantly inhibited glioma cell proliferation, as evidenced by the 5-ethynyl-2′-deoxyuridine (EdU) assay (Figure 2A; Figure S1B), and inhibited the cell cycle to the G1/S phase (Figure 2B; Figure S1C). Knockout of *TRIM22* could increase the sensitivity of GBM cells to TMZ. We selected U251MG cells with the most obvious differences in cell-cycle changes for western blot (WB) detection. WB detection of cell-cycle regulatory proteins showed that the expression of G2/M phase regulatory proteins, including cyclin E2, P-p70 S6 Kinase$^{Thr421/Ser424}$, and P-p73^{Tyr99} [21], increased under TMZ treatment and *TRIM22* knockout. In contrast, the expression of G1/S phase regulatory proteins, including cyclin B1, P-Wee1^{Ser642}, Myt 1, P-cdc2^{Tyr15}, cyclin A2, and P-Histone H3^{Ser10},[21] showed no significant differences among the groups (Figure 2C). These results suggest that TMZ and *TRIM22* can inhibit the glioma cell cycle to the G1/S phase and that *TRIM22* knockout can enhance the inhibitory effect of TMZ on the cell cycle. In addition, the Cell Counting Kit-8 (CCK-8) assay results showed that TMZ and *TRIM22* knockout could significantly reduce cell viability (Figure 2D). *In vivo*, we found that the proliferation rate of the four *TRIM22* knockout cell lines was notably lower than that of the control group (n = 10/group) 21 days after tumor implantation. Knockout of *TRIM22* combined with TMZ (5 mg/kg/day, intraperitoneally [i.p.]) provided better tumor inhibition efficiency and survival (Figures 2E and 2F; Figures S1D and S1E). In addition, we collected 92 grade II, 65 grade III, and 70 grade IV glioma specimens from the Department of Neurosurgery, Xijing Hospital, and found that patients with high TRIM22 expression had a higher Ki-67 index both in fluorescence intensity (Figure 2G) and protein levels (Figure 2H).

Our other phenotypic experiments showed that TMZ treatment did not induce apoptosis in cells; however, significant apoptosis was observed in *TRIM22*-knockout U251MG and P1 cells after TMZ treatment (Figures S1F and S2A). In addition, we found that both *TRIM22* knockout and TMZ treatment had inhibitory effects on glioma cell migration (Figures S2B and 2C), invasion (Figure S2D), and colony formation ability (Figure S2F), as evidenced by the results of the scratch, transwell, and clonogenic assays, respectively. We did not detect any senescence effect induced by TMZ treatment or TRIM22 expression in any of the cell lines used in this study (Figure S2E). Taken together, these data suggest that the knockout of *TRIM22* inhibits glioma proliferation and improves glioma cell resistance to TMZ.

TRIM22 may bind to NT5C2 and affect the RIG-I pathway

To explore how TRIM22 promotes glioma proliferation and its effect on TMZ sensitivity, we analyzed the co-immunoprecipitation (coIP) products of TRIM22 via mass spectrometry in U251MG cells (Figure 3A) and performed proteomics analysis. The results of mass spectrometry showed that the proteins most likely to bind to TRIM22 were cytosolic purine 5-nucleotidase (NT5C2), cell division cycle and apoptosis regulator protein 1 (CCAR1), cytospin-B (SPECC1),

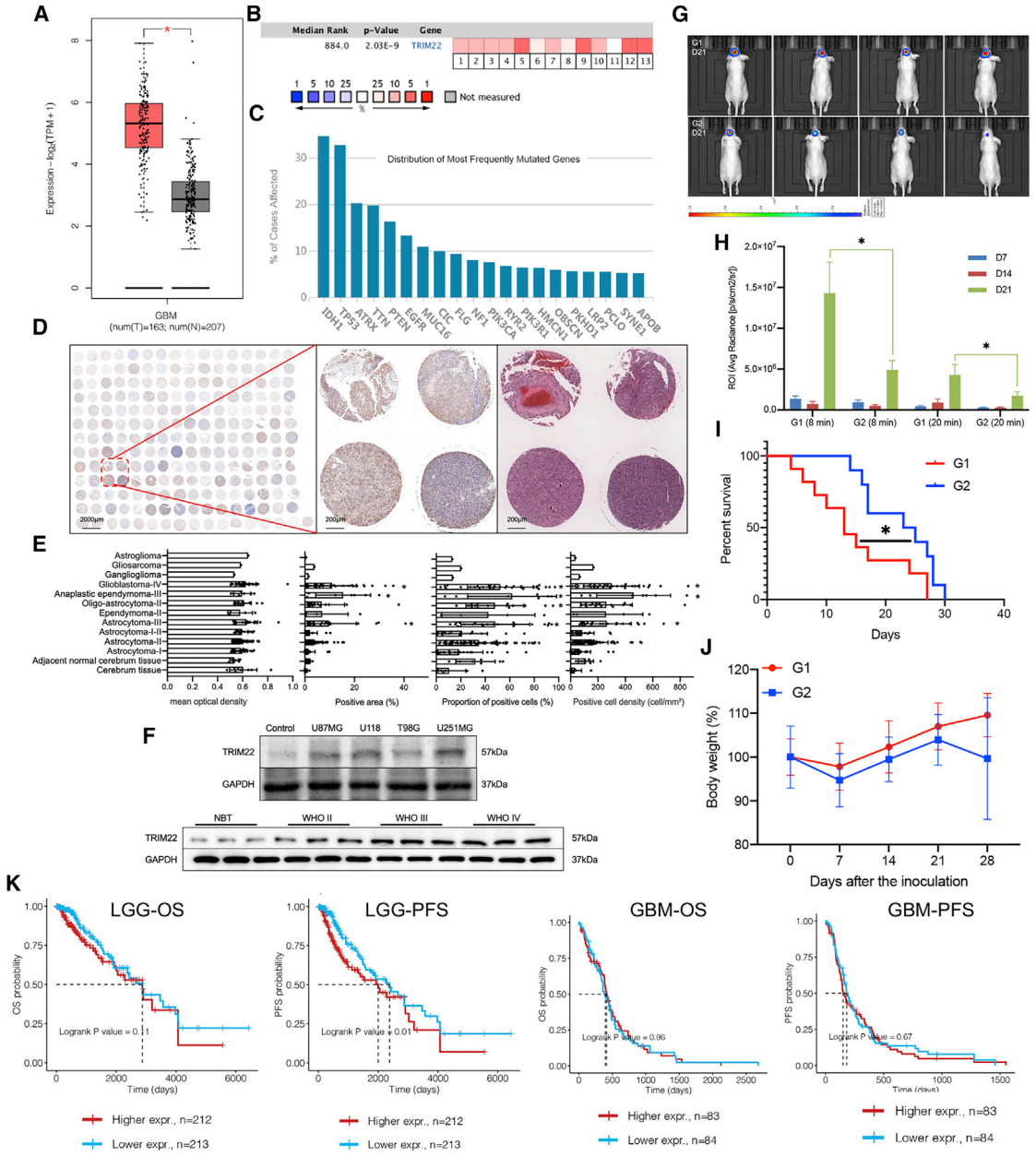

Figure 1. Expression analysis and validation of TRIM22 in different grades of gliomas

(A) Comparison of TRIM22 expression in GBM and normal tissues in GEPIA2 Database. (B) Comparison of TRIM22 expression between GBM and normal brain tissues in 13 datasets from different sources of Oncomine database. (C) The most mutated genes in GBM in the GEPIA2 database. (D) Immunohistochemical staining of TRIM22 in tissue microarrays. (E) Quantify the results of immunohistochemistry in tissue microarrays. (F) Expression of TRIM22 protein in different cell lines and clinical samples. Control, primary astrocytes; NBT, normal brain tissue. (G) *In vivo* imaging of nude mice on the 21st day after tumor implantation (8 min after intraperitoneal injection of fluorescein sodium salt). (H) Quantification of fluorescence intensity. (I) Analysis of survival rate of nude mice (log rank (Mantel Cox) test; chi square: 4.837; df: 1; p = 0.0279). (J) Comparison of body weight of nude mice. (K) Survival analysis of patients with different TRIM22 expression in GSCA database. GAPDH is used as a housekeeping protein to prove the equal loading in each lane. *p < 0.05. Each experiment was repeated three times.

PML-RARA-regulated adapter molecule 1 (PRAM1), and 60S ribosomal protein L8 (RPL8) (Figure 3B). The proteins detected via mass spectrometry were subjected to a protein interaction network analysis (Figure 3C). To predict the correlation between these proteins and GBM, we first used a database for bioinformatics analysis. The effect of the expression of each protein in different grades of gliomas on the OS and PFS of patients was searched in the GSCA database (Figure 3D). Patients with high NT5C2 and CCAR1 expression

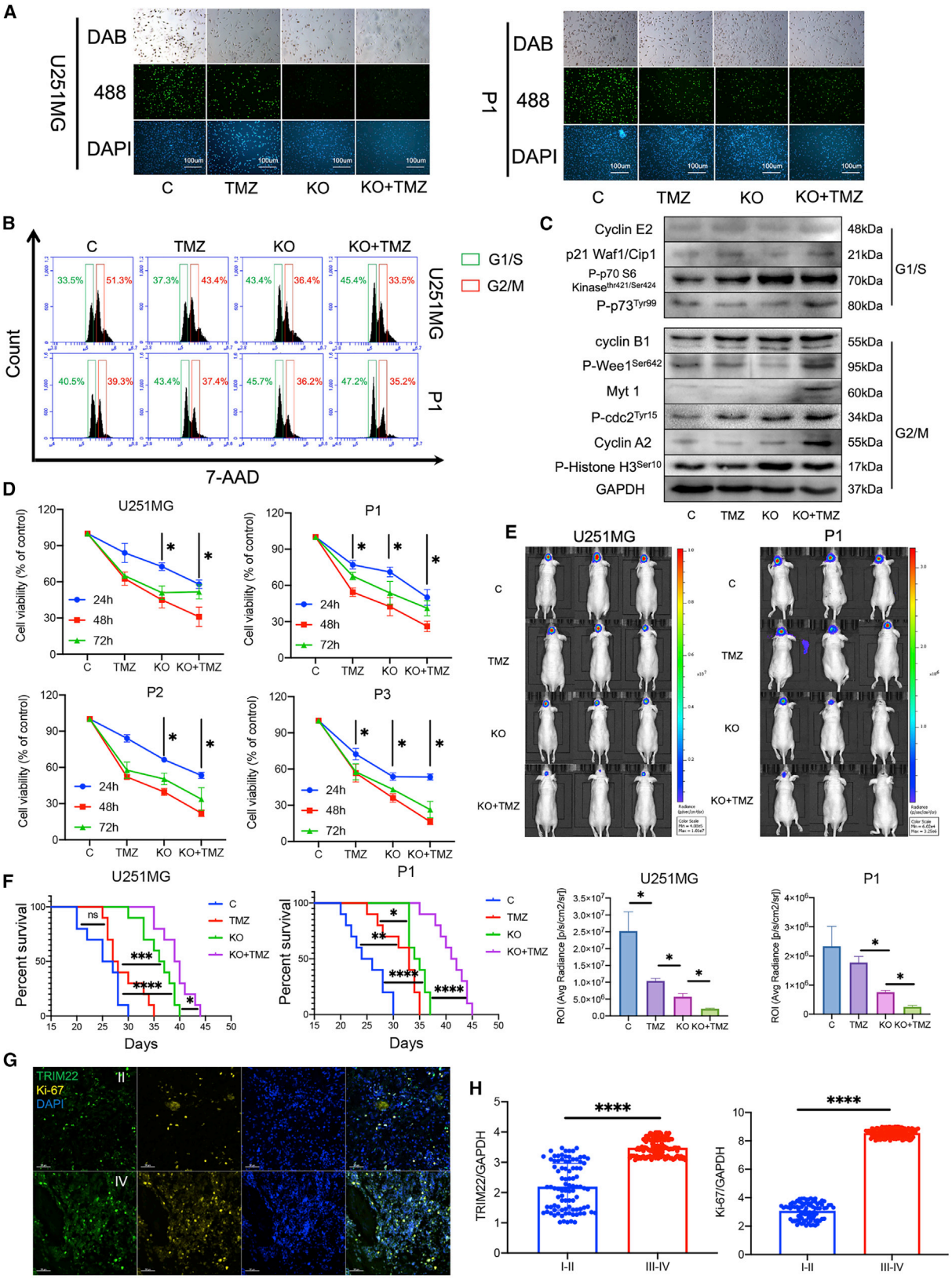

(legend on next page)

had better PFS or OS (Figures 3E–3G). However, there was no significant difference in gene transcription between the normal and GBM tissues in the GEPIA2 database (Figure 3H). In addition, data analysis from the GSCA database suggested that TRIM22, NT5C2, and CCAR1 were all enriched in pathways related to tumor proliferation and the cell cycle (Figure 3I). The results of the database suggest that there may be a potential association between these proteins. Although the conclusions of the database analysis need to be verified experimentally, these results suggest that TRIM22 may affect the NT5C2/CCAR1 pathway.

We also performed proteomic assays on differently treated U251MG cells and enrichment analysis of differentially expressed proteins (Figure 3J). KEGG results showed that the genes differentially expressed between the TMZ group and the knockout (KO) + TMZ group were mainly enriched in influenza A, herpes simplex infection, and the RIG-I signaling pathways. Influenza A and herpes simplex infection are not the main diseases in which we are interested in this study, so we chose the RIG-I signaling pathway for subsequent verification and exploration (Figure 3K; Figures S3 and S4). Taken together, these data suggest that TRIM22 may interact with NT5C2 and that the related mechanism involves the RIG-I signaling pathway.

KO of *TRIM22* inhibits the proliferation of GBM cells by reducing the expression of proteins related to the RIG-I/NF-κB/CCAR1 pathway

NF-κB is a downstream molecule of the RIG-I pathway,[22–24] and Ji et al.[18] reported that TRIM22 activates NF-κB signaling in GBM by accelerating the degradation of IκBα. To explore the effects of *TRIM22* KO and TMZ treatment on the RIG-I pathway, we performed WB for key molecules in the RIG-I/NF-κB pathway (Figure 4A). The results showed that TMZ treatment alone inhibited the expression of RIG-I, MAVS, P-IκBα^{S36}/IκBα, and NF-κB P65^{S536}/NF-κB P65. The expression of MDA-5, MAVS, P-TBK1/NAK^{Ser172}/TBK1/NAK, P-IKK-ε^{S172}/IKK-ε, P-IRF-3^{S396}/IRF-3, NF-κB P65^{S536}/NF-κB P65, and CCAR1 had a sensitizing effect on TRIM22 and TMZ (Figure S5). MAVS is a key molecule downstream of RIG-I, and its ability to bind to RIG-I represents the activation state of the RIG-I signal. We found that TMZ treatment and TRIM22 KO can inhibit the binding ability of RIG-I and MAVS and that the binding ability of RIG-I and MAVS was the weakest in the TMZ + KO group. These data suggested that TMZ and TRIM22 KO inhibited the activation of RIG-I signaling (Figure 4B).

CCAR1 plays a role in cell-cycle progression and proliferation. We found that CCAR1 expression was decreased in *TRIM22*-KO cells, as evidenced by the proteomics results (data not shown). Combined with the GTRD database and the transcription factor motifs (JASPAR CORE 2018 vertebrates) Library,[25,26] we found that NF-κB and IRF3 have a predicted binding site with CCAR1 in the region from −2,000 to 100 bp relative to the transcriptional start site (TSS) and a cutoff (p value) of 0.001 (Figure 4C). Therefore, we performed a dual-luciferase reporter assay in U251MG and 293T cells. We found that both NF-κB and IRF-3 positively regulated the transcriptional function of the CCAR1 promoter. In addition, fluorescence expression was significantly downregulated after interference with two transcription factor inhibitors, MGO (20 μM, 24 h) and si-TRIM22, indicating that both NF-κB and IRF-3 could regulate the expression of CCAR1 and that this regulatory effect was correlated with TRIM22 (Figure 4D). In addition, treatment with PPAS (20 ng/mL for 24 h), an activator of RIG-I, could activate the CCAR1 promoter in U251MG and 293T cells, while low TRIM22 expression inhibited fluorescein expression (Figure S6). Therefore, we speculate that CCAR1 is like the "effector molecule" in the RIG-I pathway that regulates the cell cycle and apoptosis.

To further validate our *in vivo* findings, nude mice (Figure 1G) were euthanized 30 days after tumor implantation. We then examined the proteins corresponding to the cellular experiments we previously performed in tissues and found that the expression levels of RIG-I, NT5C2, NF-κB, and CCAR1 were lower in the G2 group than in the G1 group (Figures 4E and 4F). In the meantime, we used a clonogenic experiment to verify its effect and found that interfering with the expression of RIG-I, NF-κB P65, or CCAR1 could significantly inhibit the glioma cell proliferation. In contrast, the overexpression of these three proteins could increase the colony number of glioma cells (Figure 4G). These results indicate that TRIM22 KO inhibits the proliferation of GBM cells by reducing the expression of proteins related to the RIG-I/NF-κB/CCAR1 pathway.

TRIM22 binds to NT5C2 as a novel E3 enzyme to ubiquitinate the RIG-I protein

To explore how TRIM22 regulates the RIG-I pathway and verify the mass spectrometry results, we conducted coIP experiments in U251MG cells to detect the binding ability between TRIM22 and NT5C2, RIG-I, CCAR1, SPECC1, PRAM1, or RPL8. The results showed that TRIM22 could interact with NT5C2 and RIG-I but could not bind to CCAR1 or other proteins (Figure 5A). Interestingly, RIG-I was not present in the mass spectrometry results but was enriched in the proteomics analysis. In addition, bimolecular fluorescent complimentary (BiFC) results showed that U251MG cells transfected with TRIM22-1/2YFP and that NT5C2-1/2YFP plasmids showed yellow

Figure 2. Knockout of *TRIM22* inhibits proliferation of GBM *in vivo* and *in vitro*

(A) The effect of TMZ (100 μM; 48 h) treatment and knockout of *TRIM22* on U251MG and P1 cell lines was examined by Edu (488 and 3,3N-diaminobenzidine tertrahydrochloride [DAB], 20×). (B) Flow cytometry was used to detect cell cycle in U251MG and P1. (C) Western detection of cell-cycle regulatory protein expression in U251MG. (D) Cell viability assay under different treatments. (E) *In vivo* imaging was performed in nude mice of different treatment groups on the 21st day after tumor implantation. (F) The survival rate of nude mice in different groups was analyzed. (G) Multiplexed immunohistochemistry was used to detect TRIM22 and Ki-67 expression in clinical samples. (H) Clinical samples were examined for TRIM22 and Ki-67 expression by RT-PCR. GAPDH is used as a housekeeping protein to prove the equal loading in each lane. *$p < 0.05$, **$p < 0.01$, ***$p < 0.001$, and ****$p < 0.0001$. Each experiment was repeated three times.

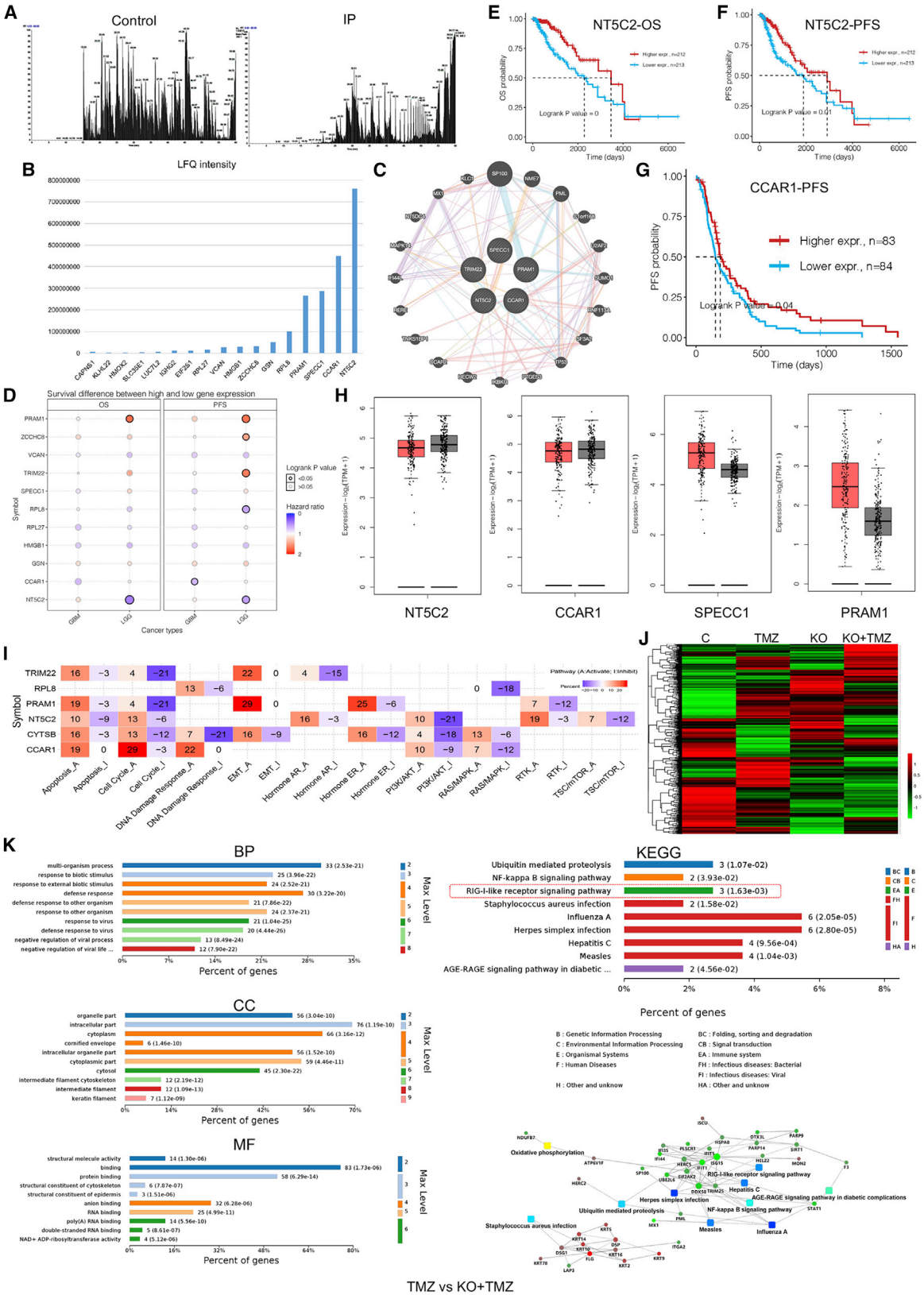

(legend on next page)

fluorescence, indicating that TRIM22 and NT5C2 were spatially close (Figure 5B).

To further investigate how the three proteins interact, U251MG cells were treated with cycloheximide (CHX; protein synthesis inhibitor) and MG132 (proteasome inhibitor). We found that TRIM22 and NT5C2 protein expression decreased significantly at 6 and 7 h after CHX treatment, respectively, while RIG-I showed a significant decrease at 4 h after treatment. This trend was reversed by the addition of MG132 (100 μM) (Figures S7A and S7B). We also found that TRIM22 KO and overexpression had no effect on the degradation of NT5C2, but TRIM22 overexpression significantly accelerated RIG-I degradation (Figure 5C). Therefore, we tentatively conclude that TRIM22 and NT5C2 regulate RIG-I ubiquitination. To explore the resulting interactions when combining the three proteins, we transfected exogenous FLAG-TRIM22, HA-NT5C2, and His-RIG-I plasmids into U251MG cells and detected the binding ability between the TRIM22 and the two other exogenous proteins using a tag antibody and an endogenous protein antibody, respectively. We found that TRIM22 could bind to NT5C2 and RIG-I both exogenously and endogenously (Figure 5D). In addition, we performed coIP assays with His-RIG-I and found that RIG-I was ubiquitinated on K48 and K63 but not on K11 or K27 (Figure 5E). Interestingly, after TRIM22 KO, the expression of NT5C2 in the pull-down component was downregulated, indicating that NT5C2 and RIG-I interacted indirectly. In addition, the trend of the K48-linked ubiquitination of RIG-I was consistent with that of NT5C2, whereas the K63-linked ubiquitination of RIG-I was consistent with that of TRIM22 (Figure 5E). These data show that NT5C2 is responsible for the K48-linked ubiquitination of RIG-I and that TRIM22 is responsible for the K63-linked ubiquitination of RIG-I.

In addition, we used FLAG-Ubi-K48 and FLAG-Ubi-K63 plasmids for reverse IP experiments. The results indicated that RIG-I was ubiquitinated at K48 and K63 (Figure S7C). We also found that RIG-I was ubiquitinated only on K48 when TRIM22 was expressed at a relatively low level. In contrast, RIG-I was ubiquitinated at K63 in the presence of low NT5C2 expression (Figure S7D). Taken together, these results suggest an interaction between TRIM22 and NT5C2. TRIM22 regulates the K63-linked ubiquitination of RIG-I, whereas NT5C2 regulates the K48-linked ubiquitination of RIG-I.

TRIM22 and NT5C2 co-regulate the RIG-I/NF-κB/CCAR1 pathway

TRIM22, as an E3 ubiquitin ligase, regulates protein ubiquitination. On the other hand, RIG-I expression is downregulated after *TRIM22* KO, which is inconsistent with the ubiquitin degradation pathway. To investigate the role of TRIM22 in this pathway after binding NT5C2, we performed a rescue experiment and found that small interfering RNA (siRNA)-mediated silencing of TRIM22 or NT5C2 significantly reduced the expression of these proteins (Figures 6A and 6B). In addition, the overexpression of TRIM22 or NT5C2 promoted the expression of RIG-I pathway proteins, but simultaneous overexpression of both did not show a stronger effect (Figures 6A and 6B). These results are not in line with our expectations because it has previously been shown that K48-linked ubiquitination is mainly responsible for protein degradation,[27] whereas K63-linked ubiquitination is mainly responsible for protein regulation and signaling.[28]

In addition, we explored the effects of TRIM22 and NT5C2 on tumor proliferation. We found that the knockdown of both TRIM22 and NT5C2 significantly inhibited the clonogenic formation of glioma cells, whereas their overexpression promoted cell proliferation (Figure 6C). However, co-knockdown or overexpression of the two proteins did not result in significant inhibition or promotion of cell proliferation (Figure 6C). To further verify that TRIM22 overexpression resulted in the increased expression and activation of RIG-I, we treated U251MG, P1, P2, and P3 cells with Cyclo, an inhibitor of RIG-I. Cyclo inhibits the post-transcriptional modification of RIG-I and reduces its ubiquitination. We found that RIG-I expression increased after 24 h of treatment with Cyclo (20 μM) in U251MG, P1, P2, and P3 (Figure S8). *In vivo*, Cyclo treatment (5 mg/kg/day, i.p.) restored the tumor growth inhibition induced by *TRIM22* KO (n = 10/group) (Figures 6D and 6E). with to the KO + TMZ group, Cyclo treatment also reduced the survival rate of nude mice (Figure 6F; Figure S9A). In addition, GTRD database analysis showed a potential binding site between TRIM22 and *CCAR1* (Figure S9B). We speculated that TRIM22 directly acts as a transcription factor of *CCAR1* to regulate *CCAR1* expression, but further verification is needed (Figure 6G). Taken together, these data suggested that TRIM22 and NT5C2 co-regulate the RIG-I/NF-κB/CCAR1 pathway.

High TRIM22 expression predicts poor prognosis in patients with GBM

To study the clinical prognosis of patients with different levels of TRIM22 expression, we collected 227 glioma specimens from patients at Xijing Hospital, including 92 cases of grade II gliomas, 65 cases of grade III gliomas, and 70 cases of grade IV gliomas. For validation, pathological diagnosis and hematoxylin and eosin staining (Figure 7A) were performed on each specimen. All fresh specimens were subjected to mRNA extraction for reverse transcription polymerase chain reaction (RT-PCR). We found that the expression levels of TRIM22, NT5C2, RIG-I, NF-κB, CCAR1, and Ki-67 were higher in

Figure 3. Mass spectrum of TRIM22 IP product and results of proteomics between different groups

(A) Total ion chromatogram of IP product mass spectrum. (B) Quantification of mass spectrometry results. (C) Protein-protein interaction (PPI) graph of protein interaction network. (D) OS and PFS analysis of proteins in mass spectrometry results in GBM and LGGs. (E) Analysis of OS by different NT5C2 expression levels in LGGs. (F) Analysis of PFS by different NT5C2 expression levels in LGGs. (G) Analysis of PFS by different CCAR1 expression levels in GBM. (H) Differential expression of NT5C2, CCAR1, SPECC1, and PRAM1 in GBM (n = 163; red) and normal tissues (n = 207, gray). (I) Protein functional enrichment in the GSCA database. (J) The heatmap of proteomics for U251MG. (K) GO/KEGG analysis between TMZ and KO + TMZ groups. Each experiment was repeated three times.

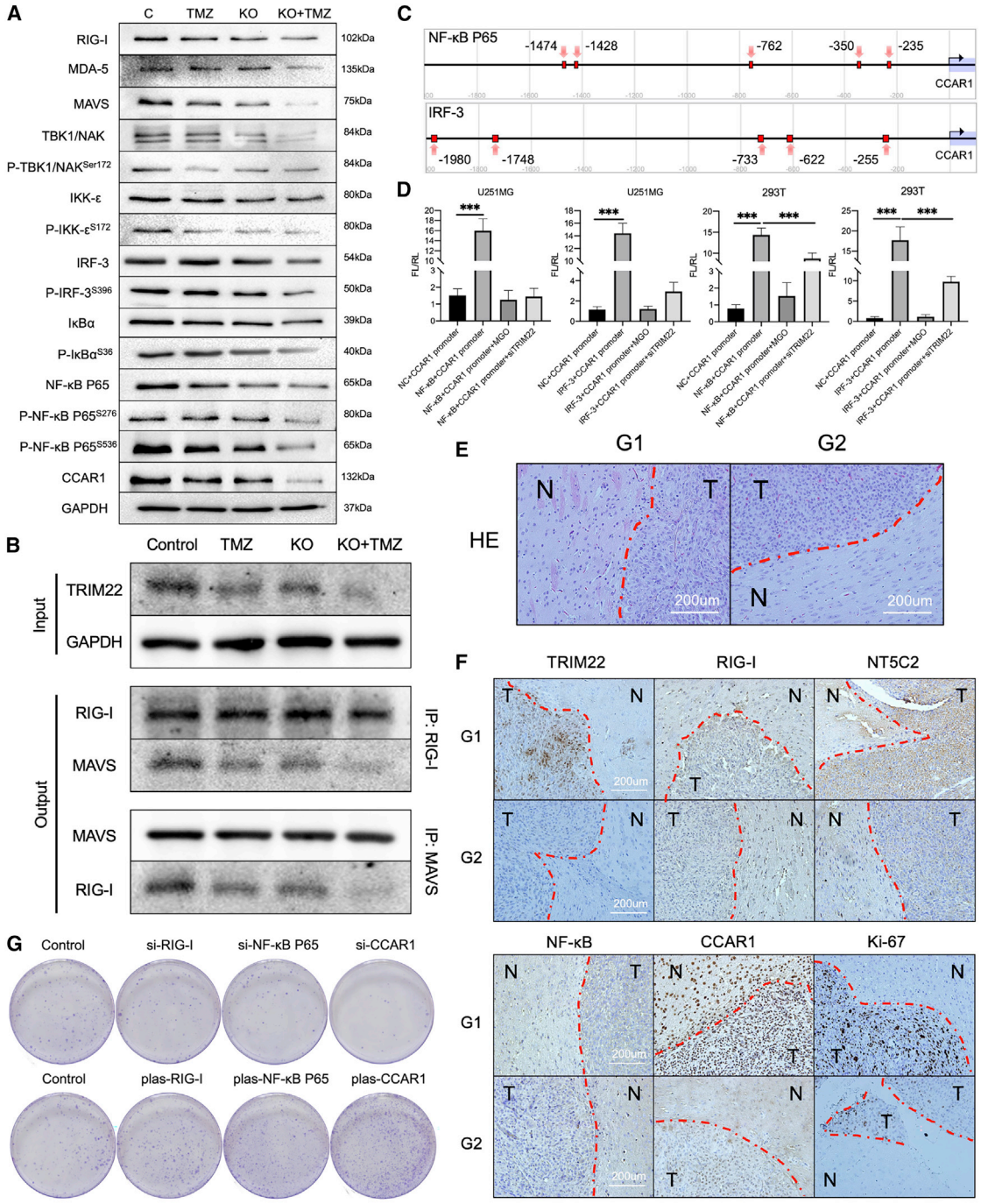

Figure 4. Knockout of *TRIM22* inhibits the expression of proteins in the RIG-I/NF-κB/CCAR1 pathway

(A) Expression of RIG-I/NF-κB/CCAR1 pathway proteins between different groups. (B) The binding ability of RIG-I and MAVS in different modified U251MG cells was detected by coIP. (C) Binding sites for the transcription factor NF-κB and IRF-3 to CCAR1 promoter. (D) Dual-luciferase reporter assay of NF-κB and IRF-3 for CCAR1-promoter. FL/RL, Firefly luciferase/Renilla luciferase. Renilla activity was used to normalize luciferase reporter activity. The promoterless firefly-luciferase vector pGL4.15 served as the negative control (NC). (E) H&E staining of mouse brain tissue sections. T, tumor; N, normal tissue. (F) Immunohistochemical staining of RIG-I/NF-κB/CCAR1 pathway in mouse brain tissue sections. T, tumor; N, normal tissue. (G) Clonogenic situation after knockdown or overexpression of RIG-I, NF-κB, and CCAR1; control on the top panel: control sequence of siRNA, invalid sequence; control of bottom panel: control sequence of overexpression plasmid, empty vector. GAPDH is used as a housekeeping protein to prove the equal loading in each lane. *$p < 0.05$ and ***$p < 0.001$. Each experiment was repeated three times.

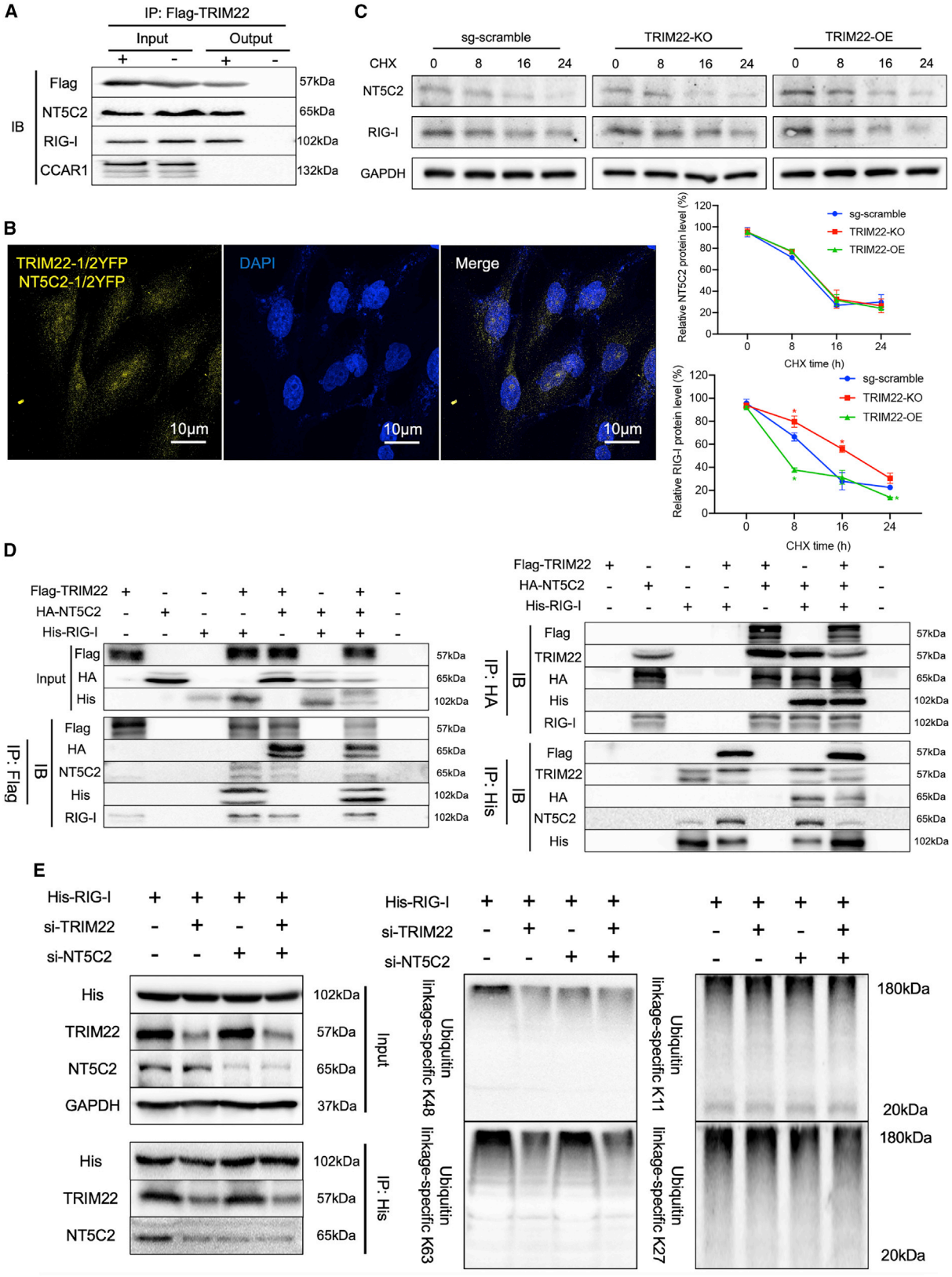

(legend on next page)

high-grade gliomas (HGGs) than in LGGs. In addition, we examined the mRNA levels of IDH-1- and MGMT-mutated genes and found no significant differences between groups (Figure 7B).

We followed up on the survival rate of these 227 patients for 10 years and received follow-up information from 110 of them, including 42 patients with grade II gliomas, 36 patients with grade III gliomas, and 32 patients with grade IV gliomas. All patients on whom we received follow-up information died of glioma. Patients with HGG had a shorter survival time than those with LGG (Figure 7C). Specimens of the same grade were divided into TRIM22-high and -low expression groups using the median as the boundary. The results showed that patients with low TRIM22 expression had better survival in HGG (Figure 7D), which was not consistent with the results of the database analysis (Figure 1K). In addition, co-localization of TRIM22, NT5C2, and RIG-I occurred in both grade II and IV gliomas, which also illustrates, to some extent, the interaction between the three proteins and corresponds to the coIP results (Figure 7K). We also performed multiplex fluorescence immunohistochemical experiments and found that the expressions of TRIM22, NT5C2, RIG-I, NF-κB, and CCAR1 were lower in LGG than that in HGG (Figure 7F). No significant differences were observed in the expression of IDH-1 and MGMT. To explore the effect of TRIM22 expression on the efficacy of TMZ treatment, we divided the patients into three groups: no chemotherapy, TMZ, and nimustine. According to their TRIM22 expression, the patients were divided into a high expression group (+) and a low expression group (−). We found that patients with low TRIM22 expression had higher survival rates after TMZ treatment (Figure 7G). Taken together, these data suggest that TRIM22 predicts a higher grade of human glioma malignancy and that TMZ has a better effect on patients with low TRIM22 expression.

DISCUSSION

Our study found that TRIM22 was highly expressed in GBM cells. KO of *TRIM22* inhibits the proliferation of GBM cells and improves TMZ sensitivity in gliomas. TRIM22, a member of the TRIM family of proteins, may act as a new E3 ubiquitin ligase after binding NT5C2 in GBM. The TRIM22-NT5C2 complex is responsible for the K63- and K48-linked ubiquitination of RIG-I, affecting the downstream NF-κB pathway. Moreover, NF-κB regulates the expression of CCAR1, thereby increasing tumor proliferation.

RIG-I is mainly responsible for transmitting downstream signals, owing to the two repetitive caspase activation and recruitment domains (CARDs) at its N terminus.[29] The involvement of the RIG-I/NF-κB pathway has been reported in various diseases.[24,30,31] Surprisingly, CCAR1 could not bind to TRIM22, while RIG-I bound to TRIM22. This demonstrates the uncertainty of high-throughput sequencing and the need for verification experiments. In the rescue experiments evaluated via coIP, we found that TRIM22 knockdown led to a decrease in the amount of NT5C2 in the IP product (Figure 5E). We believe that not all NT5C2 may directly bind to RIG-I based on the spatial structure analysis. Moreover, there is a part of NT5C2 that only binds to TRIM22 and affects RIG-I by regulating the ubiquitin ligase function of TRIM22 (Figure 6G). From the perspective of protein function, whether NT5C2 functions as an E3 ubiquitin ligase remains unknown, as NT5C2 may only play a "flavoring agent" role on TRIM22. NT5C2, without TRIM22, could not regulate or interact with RIG-I. In addition, indirect binding between the two is inevitable, as we have observed in our *in vivo* experiments. Further exploring this phenomenon using an *in vitro* IP assay, EMSA, or yeast one-hybrid system can better prove our conclusions.

To ensure the use of the same class of genetic engineering technologies in the same experiment, we utilized interfering RNA and CRISPR-Cas9 technologies, respectively, to knock down and knock out *TRIM22*. However, we found that two different disposal methods had different effects on downstream RIG-I/NF-κB pathway proteins. Although the downregulation of TRIM22 expression induced by different ways inhibited the activation of RIG-I/NF-κB pathway and reduced the expression of pathway-related proteins, the expression regulation effect of TRIM22-KO was more obvious than knockdown TRIM22 (Figures 4A and 6A). In addition, in the exploration experiment of TRIM22 on the phenotype of GBM cells, we also observed that the same treatment had different effects in cells from different sources. Therefore, in the follow-up mechanism exploration experiment, we selected U251MG cells with the most prominent phenotypic results for the experiment. This also explains why the results of the database are different or even opposite to what we predicted. It may also be because the GBM samples and cells used are different. In addition, Ji et al.[18] found that the overexpression of TRIM22 could accelerate the degradation of IκBa in U87MG, U118MG, and LN229 cells, which was inconsistent with our results in U251MG. The conflicting results of these different studies further confirm the importance of personalized treatment of GBM in clinic.

Protein expression of the RIG-I/NF-κB pathway was downregulated after NT5C2 or TRIM22 knockdown, whereas overexpression of both NT5C2 and TRIM22 upregulated it (Figure 6A). This phenomenon cannot be explained by the theory that K48-linked ubiquitination is mainly responsible for protein degradation.[32] Therefore, we speculated that although TRIM22 and NT5C2 are responsible for

Figure 5. coIP results of TRIM22-binding protein and ubiquitination of RIG-I

(A) IP results for TRIM22 binding to NT5C2, RIG-I, and CCAR1 (+: pulldown antibody was added, −: immunoglobulin G [IgG] was added; output: product after pulldown). (B) BiFC experiments for TRIM22 and NT5C2. (C) Differently modified U251MG was treated with CHX at a concentration of 100 μM for different periods of time, and WB was used to detect the expression of NT5C2 and RIG-I proteins. (D) Western blot of IP incubated with anti-FLAG, anti-HA, anti-His, anti-TRIM22, anti-NT5C2, and anti-RIG-I antibodies to detect the combination of TRIM22, NT5C2, and RIG-I in U251MG cells. (E) Ubiquitination assay of RIG-I in U251MG cells. To assess *in vivo* ubiquitination, modified cells were treated with 20 μM MG132 for 6 h before lysis, followed by coIP and WB analysis. GAPDH is used as a housekeeping protein to prove the equal loading in each lane. *$p < 0.05$. Each experiment was repeated three times.

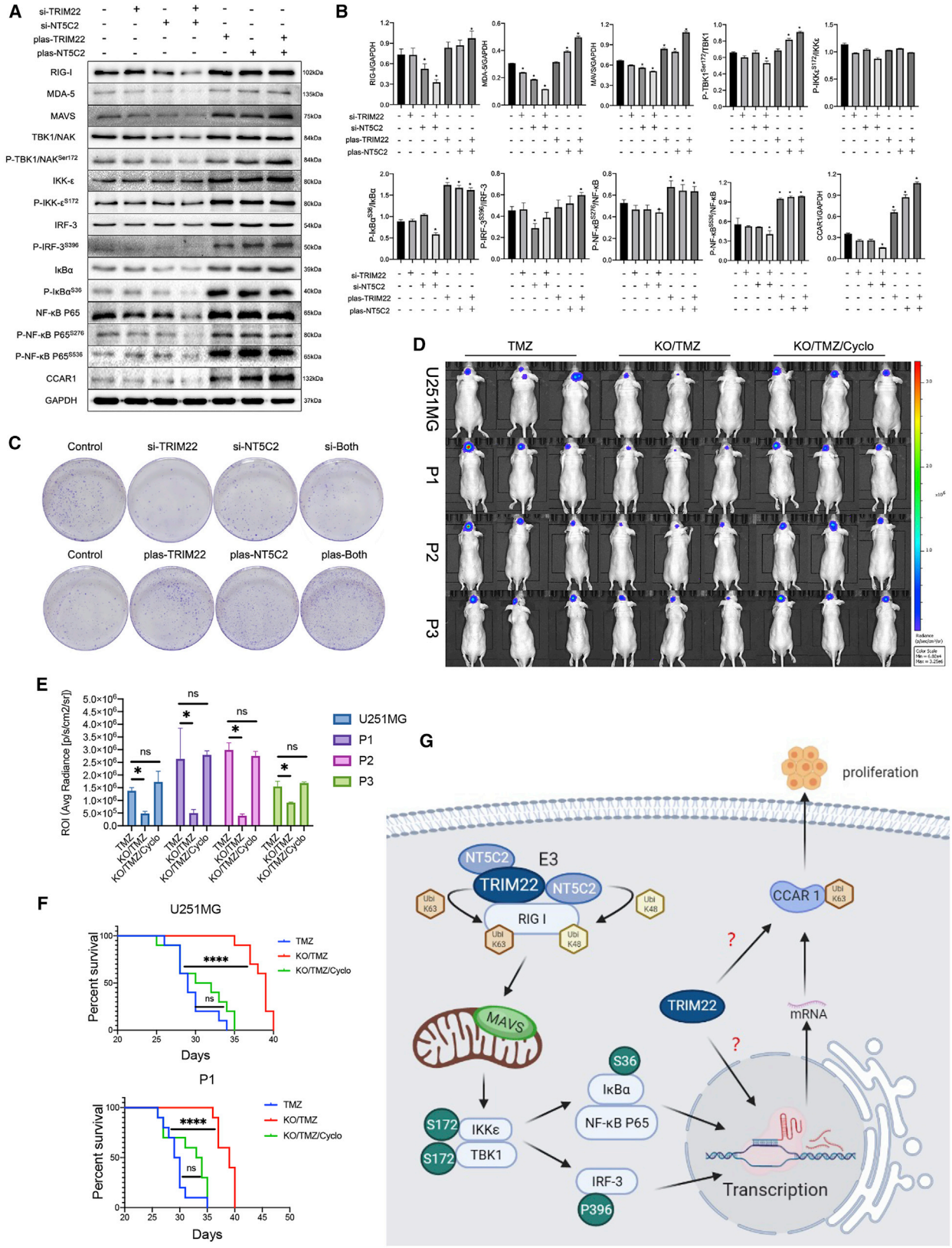

(legend on next page)

the K48- and K63-linked ubiquitination of RIG-I, the function exerted by TRIM22-NT5C2 is related to its total expression level. The amount of protein expression that leads to changes in protein function is referred to as the "baseline value" of the protein. Below the baseline value, RIG-I was mainly regulated by the K48-linked ubiquitination responsible for NT5C2. At expression levels higher than the baseline, RIG-I is mainly regulated by K63-linked ubiquitination, which is responsible for TRIM22. Hence, our findings may revolutionize the clinical use of targeted drugs. At present, the use of clinically targeted drugs is mainly aimed at determining whether patients have targeted genetic mutations or changes in gene expression, regardless of the choice of medication after quantifying the target indicators. Therefore, patients undergoing targeted drug therapy need to be more carefully classified according to the baseline values of specific target proteins to determine if inhibitors or agonists of the targeted molecule should be used. In addition, this theory may also explain why patients who meet the criteria for targeted drug therapy always experience different efficacies after medication. In addition to individual differences between patients, this effect may be explained by differences in the mechanism of drug action. Unfortunately, more studies are needed to explore whether there is a baseline value for the target genes of various types of targeted drugs, as well as how to measure the baseline value for these genes.

In summary, our study identified a novel regulatory mechanism of TRIM22 in GBM. The discovery of the TRIM22-NT5C2/RIG-I/NF-kB/CCAR1 pathway offers new hope for multi-target combination therapy for GBM and improves the benefits of TMZ. In addition, the possibility of the existence of baseline values also provides a new direction for subsequent tumor-targeted research, more than just gliomas.

MATERIALS AND METHODS

Ethics approval and consent to participate

Ethical approval was obtained from the Xijing Hospital Research Ethics Committee, and written informed consent was obtained from each patient. All experimental procedures were approved by the Institutional Animal Care and Use Committee of Fourth Military Medical University. Moreover, this study was performed in accordance with the principles of the Declaration of Helsinki.

Cell culture and experimental groups

The U251MG, U118, T98MG, U87MG, and 293T cell lines were purchased from Genechem (Shanghai, China). The P1, P2, and P3 cell lines were obtained from human glioma specimens. All cell lines were identified via STR analysis, and mycoplasma detection was performed. Cells were cultured in DMEM (Corning, cat. no. 10-013-CVR) containing 10% fetal bovine serum (FBS) (Gibco, cat. no. 10099141). The culture flasks were then placed in a cell incubator at 37°C and 5% CO_2. The conditions of cells treated with TMZ were designed as follows: TMZ (100 μM) was added to the cells, and they were cultured for another 48 h. We also used TMZ (100 μM, 48 h) as a positive control treatment group to explore its effect on glioma cell lines after knocking out *TRIM22* by CRISPR-Cas9 technology and whether TRIM22 has a sensitizing effect on TMZ. All phenotypic experiments were divided into four groups: control (C), TMZ (TMZ), *TRIM22*-KO group (KO), and *TRIM22*-KO + TMZ group (KO + TMZ).

Reagents

Anti-cyclin A2 antibody (cat. no. 4656); anti-cyclin E2 (cat. no. 4132); anti-p21 Waf1/Cip1 (cat. no. 2947); anti-phospho-histone H3 (Ser10) (cat. no. 3377); anti-Phospho-Wee1 (Ser642) (cat. no. 4910); anti-Myt1 (cat. no. 4282); anti-phospho-cdc2 (Tyr15) (cat. no. 4539); anti-cyclin B1 (cat. no. 12231); anti-phospho-p70 S6 kinase (Thr421/Ser424) (cat. no. 9204); anti-phospho-p73 (Tyr99) (cat. no. 4665); anti-GAPDH (cat. no. 5174); anti-Bax (cat. no. 2772); anti-Bcl-2 (cat. no. 3498); anti-Caspase 9 (cat. no. 9502); anti-Caspase 3 (cat. no. 9662); anti-Caspase 8 (cat. no. 9746); anti-IκB alpha (cat. no. 4814); and a RIG-I Pathway Antibody Sampler Kit (cat. no. 8348) were purchased from Cell Signaling Technology (Boston, MA, USA). Anti-IκB-α alpha (phospho S36) (cat. no. ab133462); anti-NF-κB p65 (cat. no. ab16502); anti-NF-κB p65 (phospho S276) (cat. no. ab183559); anti-NF-κB p65 (phospho S536) (cat. no. ab76302); anti-TRIM22 (cat. no. ab224059); anti-NT5C2 (cat. no. ab96084); anti-RIG-I/DDX58 (cat. no. ab45428); anti-Ki67 (cat. no. ab16667); anti-DIS (CCAR1) (cat. no. ab70243); anti-DDDDK (cat. no. ab205606), anti-HA tag (cat. no. ab236632); anti-His (cat. no. ab213204); anti-ubiquitin (linkage-specific K48) (cat. no. ab140601); and anti-ubiquitin (linkage-specific K63) (cat. no. ab179434) antibodies were purchased from Abcam (Cambridge, UK). CHX was purchased from PlantChemMed (PCM) Biology (Shanghai, China). MG132 (cat. no. HY-13259), Cyclo (cat. no. HY-P1934), polyinosinic polycytidylic acid sodium (PPAS) (cat. no. HY-135748), and malachite green oxalate (MGO) (cat. no. HY-D0162) were purchased from MedChemExpress (Shanghai, China). The GoldHi EndoFree Plasmid Maxi Kit (CW2104M) was purchased from Beijing ComWin Biotech. A five-color multiple fluorescence immunohistochemical staining kit was purchased from Shanghai Absin Biotech (cat. no. abs50013). HiScript II Q Select RT SuperMix for qPCR (+gDNA wiper) (cat. no. R233-01) and ChamQ SYBR Color qPCR Master Mix (Low ROX Premixed) (cat. no. Q431-02) were purchased from Vazyme Biotech (Nanjing, China). TMZ (cat. no. 76899) was purchased from Sigma-Aldrich (St. Louis, MO, USA).

Figure 6. Regulation of RIG-I/NF-κB/CCAR1 pathway by TRIM22 and NT5C2

(A) Expression of RIG-I pathway protein under different siRNA and overexpression plasmid treatments. (B) Quantification of results in (A). (C) Clonogenic situation after knockdown or overexpression of TRIM22 and NT5C2. (D) *In vivo* imaging was performed on the 21st day after tumor implantation from different origins (n = 10/group). Cyclo (5 mg/kg/day, i.p.); TMZ (5 mg/kg/day, i.p.). (E) Quantification of region of interest (ROI) in (D). (F) Survival analysis of U251MG and P1 implanted mice. (G) Molecular mechanism diagram. GAPDH is used as a housekeeping protein to prove the equal loading in each lane. ns, not significant, *$p < 0.05$, and ****$p < 0.0001$. Each experiment was repeated three times.

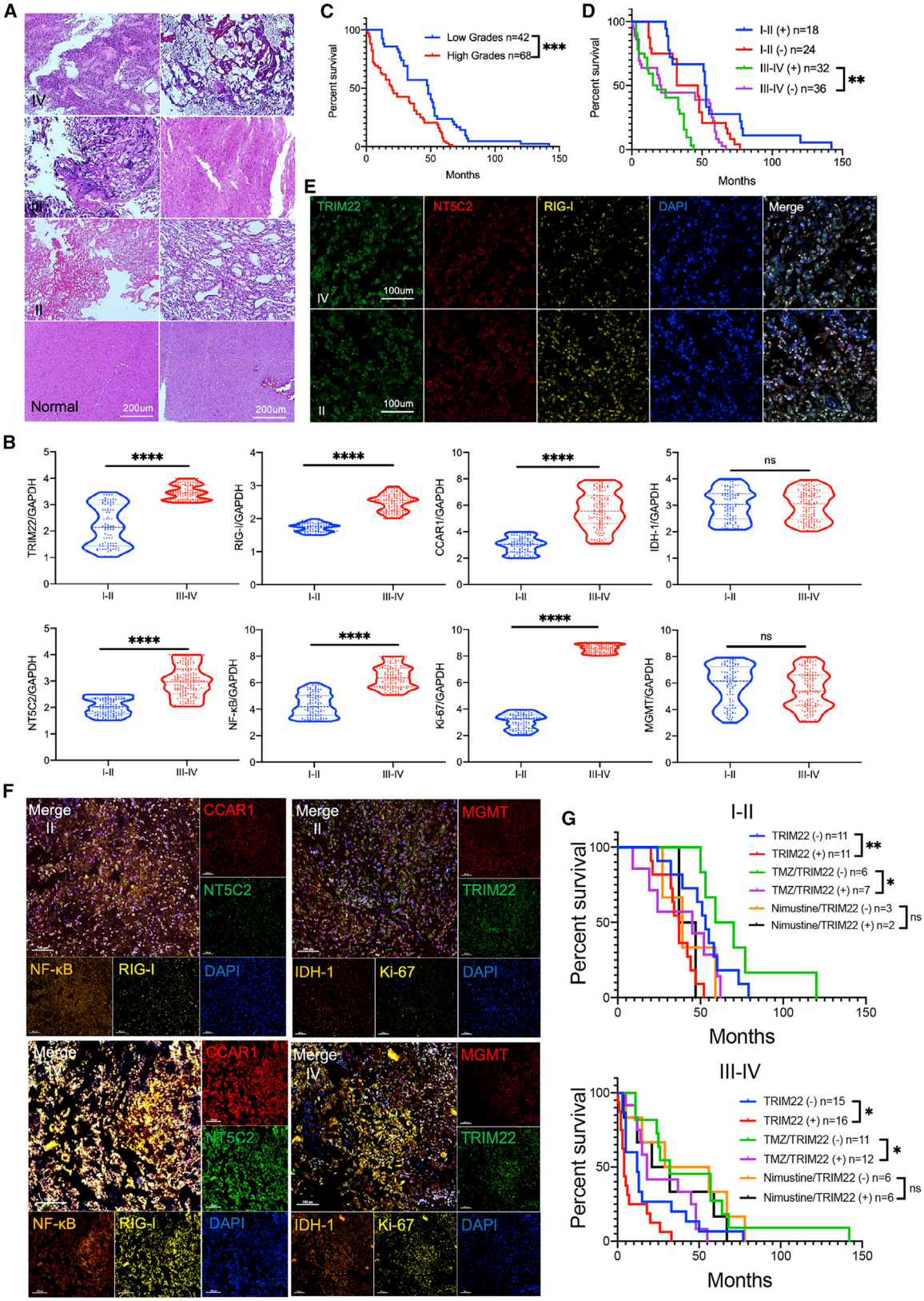

(legend on next page)

Lentiviral infection, transient transfection, and Cas9/sgRNA KO

The plasmids and siRNAs were transfected into cells by using jetPRIME reagent (Polyplus). The experimental operation was carried out in strict accordance with the instructions of the transfection reagent manufacturer. The Leti-Cas9-puro and single-guide RNA (sgRNAs) lentiviruses were designed and constructed by Genechem (Shanghai, China). Lentivirus containing Cas9 and sgRNAs were introduced into U251MG, P1, P2, and P3 cells. Forty-eight hours after infection, the cells were cultured in fresh medium containing Puro for 15 days to screen the cells with stable expression. All plasmids were designed and constructed by Hanbio (Shanghai, China). Sequences of sgRNAs for CRISPR-Cas9 and shRNA are listed in Table S2.

Flow cytometry analysis of the cell cycle and apoptosis, cell scratch assay, cell invasion assay, cell clonogenic experiment, CCK-8 assay, immunofluorescence (IF), immunohistochemistry (IHC), coIP, and WB.

All these experiments were performed as previously described.[21,33] Tissue arrays were purchased from Alenabio Biotechnology (Xi'an, China).

Cell senescence experiment

A cell senescence β-galactosidase staining kit was purchased from Beyotime (cat. no. C0602). Briefly, the cells were cultured in a 6-well plate for appropriate cell density, and the cells in each well were treated according to the experimental groups. The spent cell culture medium was removed, the cells were washed once with PBS, 1 mL β-galactosidase staining fixative was added, and the cells were fixed at room temperature (25°C) for 15 min. The cell fixation solution was then removed, and the cells were washed three times with PBS for 3 min each time. The working solution was prepared according to the manufacturer's protocol, the PBS used for washing was removed, and 1 mL working staining solution was added to each well. The cells were then incubated overnight at 37°C, and the plates were covered with a plastic wrap to prevent evaporation. The senescent cells were observed and counted under an ordinary light microscope.

Relative quantitative analysis of the proteome based on TMT

U251MG cells with different modifications were collected for proteomics. In addition, the modified cells were collected in a 1.5 mL EP tube, and 1 mL ice-cold RIPA buffer (Sigma-Aldrich, St. Louis, MO, USA) was added. The cells were lysed on ice for 15 min. Two μg primary anti-TRIM22 antibody was added and incubated for 1 h at 4°C. Twenty μL resuspended volume of Protein A/G PLUS-Agarose (SANTA CRUZ, Shanghai, China) was added. The tubes were capped and incubated at 4°C on a rotating device overnight. Immunoprecipitates were collected by centrifugation at 2,500 RPM for 5 min at 4°C. We carefully aspirated and discarded the supernatant. The pellet was washed 4 times with 1.0 mL PBS, each time repeating the centrifugation step above. After a final wash, the supernatant was aspirated and discardd, and the pellet was in 40 μL 1× electrophoresis sample buffer. The pull-down products collected were used for mass spectrometry. Mass spectrometric detection of the coIP products was performed by Beijing Bio-Tech Pack Technology.

RT-PCR

The TRIzol method was used to extract and quantify RNA from tissues. Reverse transcription was performed according to the protocol of the Hiscript II Q Select RT Supermax for qPCR (+ gDNA wiper) kit. Next, qPCR was performed using a Chamq SYBR Color qPCR Master Mix (Low ROX Premixed) kit, following the manufacturer's protocol. The mRNA expression of the genes of interest were calculated using the $2^{-\Delta\Delta Ct}$ method, and GAPDH was used as an internal control. Primers were designed and synthesized by Takara Bio. The primer sequences used are listed in Table S3.

BiFC experiments

TRIM22-1/2YFP and NT5C2-1/2YFP plasmids were constructed and sequenced by Shanghai Genechem. The plasmids were transfected into U251MG cells using jetPRIME reagent (Polyplus). The cells were then cultured for 8 h, then the spent medium was replaced with fresh culture medium. After 24 h, the expression level of the yellow fluorescent protein in the U251MG cells was observed under a confocal microscope.

Dual-luciferase reporter assay

The CCAR1 promotor firefly luciferase, transcription factor expression plasmid, and Renilla reporter constructs were designed and constructed by Genechem (Shanghai, China).

Plasmids were co-transfected into modified U251MG and 293T cells using a Polyplus/jetPRIME kit. Twenty-four hours after transfection, the regulatory effects of the transcription factors and target gene promoters were detected using a dual-luciferase assay kit (Promega, cat. no. E1910), and the experimental procedures were performed according to the manufacturer's instructions. Cells were analyzed in three wells per experiment to obtain average counts and in three independent biological replicates.

Mouse intracranial tumor model and bioluminescence detection

All animal experiments were conducted according to the protocols approved by the Institutional Ethics Committee of Xijing Hospital, Fourth Military Medical University. All nude mice were purchased

Figure 7. Expression and survival analysis of TRIM22 in clinical patients

(A) H&E staining of different grades of glioma (10×). (B) Expression of RIG-I/NF-κB/CCAR1 pathway mRNA in HGGs and LGGs. (C) Survival analysis of GBM and LGGs. (D) Survival analysis of LGGs and GBM with different TRIM22 expression. (E) Co-expression of TRIM22, NT5C2, and RIG-I in different grades of glioma (20×). (F) Expression of TRIM22, NT5C2, RIG-I, NF-κB, CCAR1, Ki-67, IDH-1, and MGMT in grade II (40×) and IV gliomas (40×). (G) The survival rate of patients with different TRIM22 expression levels in different treatment groups was analyzed. Ns, not significant, *$p < 0.05$, **$p < 0.01$, ***$p < 0.001$, and ****$p < 0.0001$. Each experiment was repeated three times.

from Shenzhen Huafukang Bioscience (Shenzhen, China). Mice were anesthetized via i.p. injection with 4% chloral hydrate, and the perianal temperature of the mice was maintained at 37°C. Each mouse was fixed on a stereotactic device, the skin of the mouse head was disinfected, the skull was exposed, and a small hole was made in the right of the skull using a grinding wheel (2 mm posterior and 1 mm lateral to the bregma). Tumor cells (3×10^6 cells/5 μL PBS) were injected within 2 min into the mouse brain (depth: 2.8 mm) using a micro-syringe. The syringe was left in the skull for 5 min to prevent cell leakage. After the operation, the skull was sealed with bone wax, the incision was sutured, and glucose (0.5 mL) was injected into the abdominal cavity. Fluorescence bioluminescence detection equipment (IVIS Lumina III) was used to detect tumor formation at different time points after surgery.

Datebase analyses

The GEPIA2 database (http://gepia2.cancer-pku.cn/) was used to compare TRIM22 mRNA expression in different tumor and normal control tissues. Oncomine (https://www.oncomine.org) was used to compare TRIM22 expression in GBM and normal brain tissues using datasets from different sources. To compare the survival rates of patients with different TRIM22 expression levels, the GSCA database (http://bioinfo.life.hust.edu.cn/web/GSCALite/) was used. The GTRD database (http://gtrd.biouml.org) was used to analyze potential sites for protein-DNA binding. The STRING database (https://string-db.org/) was used to retrieve possible potential interactions between proteins.

Statistics

All experiments were repeated three times, and SPSS software (v.26.0) was used for data analysis. The Shapiro-Wilk test was used to determine whether the data had a normal distribution. Experimental data conforming to the normal distribution are expressed as the mean ± standard deviation. Two samples that conformed to a normal distribution were compared using the t test. Multiple sample comparisons were performed using one-way analysis of variance (ANOVA). $p < 0.05$ was considered statistically significant.

SUPPLEMENTAL INFORMATION

Supplemental information can be found online at https://doi.org/10.1016/j.omto.2022.08.007.

ACKNOWLEDGMENTS

The work was supported by National Natural Science Foundation of China (grant no. 81872049).

AUTHOR CONTRIBUTIONS

X.F., X.W., and Y.-N.D. designed the study, performed the experiments, and prepared the manuscript, and they contributed equally to this work. K.S., Q.G., and L.Z. were involved in experiment performance and data collection. S.L., J.W., Y.H., and X.H. made contributions to follow up with the patient and the acquisition of data. X.F. wrote the original draft. Z.F. was responsible for the supervision of the entire project and was involved in the study design, data interpretation, and manuscript preparation. All authors read and approved the final manuscript.

DECLARATION OF INTERESTS

The authors declare that they have no competing interests.

REFERENCES

1. Laws, E.R., Parney, I.F., Huang, W., Anderson, F., Morris, A.M., Asher, A., Lillehei, K.O., Bernstein, M., Brem, H., Sloan, A., et al. (2003). Survival following surgery and prognostic factors for recently diagnosed malignant glioma: data from the Glioma Outcomes Project. J. Neurosurg. *99*, 467–473.
2. Lee, E.S., Ko, K.K., Joe, Y.A., Kang, S.G., and Hong, Y.K. (2011). Inhibition of STAT3 reverses drug resistance acquired in temozolomide-resistant human glioma cells. Oncol. Lett. *2*, 115–121.
3. Xiao-Xing, L.I., Wang, Z.M., Zuo, J.L., Qi-Nian, X.U., Wang, X.Y., and Tao, C. (2007). Establishment of drug-resistance cell line of human glioma induced by temozolomide and reversion of drug-resistance. Suzhou Univ. J. Med. Sci. *27*, 169–171.
4. Yamanaka, R. (2009). Molecular-targeted therapy for malignant glioma. Brain Nerve *61*, 177–188.
5. von Deimling, A., Louis, D.N., von Ammon, K., Petersen, I., Wiestler, O.D., and Seizinger, B.R. (1992). Evidence for a tumor suppressor gene on chromosome 19q associated with human astrocytomas, oligodendrogliomas, and mixed gliomas. Cancer Res. *52*, 4277–4279.
6. Chang, C.Y., Kuan, Y.H., Ou, Y.C., Li, J.R., Wu, C.C., Pan, P.H., Chen, W.Y., Huang, H.Y., and Chen, C.J. (2014). Autophagy contributes to gefitinib-induced glioma cell growth inhibition. Exp. Cell Res. *327*, 102–112.
7. Koukourakis, G.V. (2012). Has bevacizumab (avastin) given extra therapeutic gain in metastatic colorectal cancer and malignant brain gliomas? Systematic review answering this question. Recent Pat. Inflamm. Allergy Drug Discov. *6*, 70–77.
8. Irani, S.R., Gelfand, J.M., Bettcher, B.M., Singhal, N.S., and Geschwind, M.D. (2014). Effect of rituximab in patients with leucine-rich, glioma-inactivated 1 antibody-associated encephalopathy. JAMA Neurol. *71*, 896–900.
9. Groves, M.D., Puduvalli, V.K., Hess, K.R., Jaeckle, K.A., Peterson, P., Yung, W.K.A., and Levin, V.A. (2002). Phase II trial of temozolomide plus the matrix metalloproteinase inhibitor, marimastat, in recurrent and progressive glioblastoma multiforme. J. Clin. Oncol. *20*, 1383–1388.
10. Dresemann, G. (2004). Imatinib (STI571) plus hydroxyurea: safety and efficacy in pre-treated, progressive glioblastoma multiforme (GBM) patients (pts). J. Clin. Oncol. *22* (suppl), 1550.
11. Shuang, F., Chen, Z., Qiu, W., Cai, X., Lu, J., Ning, L., Wang, H., and Neurosurgery, D.O. (2018). TRIM22 promotes proliferation, invasion and migration of glioblastoma by regulating PI3K/AKT signaling (Acta Universitatis Medicinalis Nanjing(Natural Science)).
12. Hattlmann, C.J., Kelly, J.N., and Barr, S.D. (2012). TRIM22: a diverse and dynamic antiviral protein. Mol. Biol. Int. *2012*, 153415.
13. Obad, S., Olofsson, T., Mechti, N., Gullberg, U., and Drott, K. (2007). Expression of the IFN-inducible p53-target gene TRIM22 is down-regulated during erythroid differentiation of human bone marrow. Leuk. Res. *31*, 995–1001.
14. Ding, L.H., Park, S., Peyton, M., Girard, L., Xie, Y., Minna, J.D., and Story, M.D. (2013). Distinct transcriptome profiles identified in normal human bronchial epithelial cells after exposure to γ-rays and different elemental particles of high Z and energy. BMC Genomics *14*, 372.
15. Chen, C., Zhao, D., Fang, S., Chen, Q., Cheng, B., Fang, X., and Shu, Q. (2017). TRIM22-Mediated apoptosis is associated with bak oligomerization in monocytes. Sci. Rep. *7*, 39961.
16. Duan, Z., Gao, B., Xu, W., and Xiong, S. (2008). Identification of TRIM22 as a RING finger E3 ubiquitin ligase. Biochem. Biophys. Res. Commun. *374*, 502–506.
17. Zhang, L., Zhang, B., Wei, M., Xu, Z., Kong, W., Deng, K., Xu, X., Zhang, L., Zhao, X., and Yan, L. (2020). TRIM22 inhibits endometrial cancer progression through the NOD2/NF-κB signaling pathway and confers a favorable prognosis. Int. J. Oncol. *56*, 1225–1239.

18. Ji, J., Ding, K., Luo, T., Zhang, X., Chen, A., Zhang, D., Li, G., Thorsen, F., Huang, B., Li, X., and Wang, J. (2021). TRIM22 activates NF-κB signaling in glioblastoma by accelerating the degradation of IκBα. Cell Death Differ. *28*, 367–381.

19. Yu, Z., Chen, Y., Wang, S., Li, P., Zhou, G., and Yuan, Y. (2018). Inhibition of NF-κB results in anti-glioma activity and reduces temozolomide-induced chemoresistance by down-regulating MGMT gene expression. Cancer Lett. *428*, 77–89.

20. Petersson, J., Ageberg, M., Sandén, C., Olofsson, T., Gullberg, U., and Drott, K. (2012). The p53 target gene TRIM22 directly or indirectly interacts with the translation initiation factor eIF4E and inhibits the binding of eIF4E to eIF4G. Biol. Cell *104*, 462–475.

21. Fei, X., Wang, J., Chen, C., Ding, B., Fu, X., Chen, W., Wang, C., and Xu, R. (2019). Eupatilin inhibits glioma proliferation, migration, and invasion by arresting cell cycle at G1/S phase and disrupting the cytoskeletal structure. Cancer Manag. Res. *11*, 4781–4796.

22. Nie, L., Zhang, Y.S., Dong, W.R., Xiang, L.X., and Shao, J.Z. (2015). Involvement of zebrafish RIG-I in NF-κB and IFN signaling pathways: insights into functional conservation of RIG-I in antiviral innate immunity. Dev. Comp. Immunol. *48*, 95–101.

23. Zeng, Y., Wang, P.H., Zhang, M., and Du, J.R. (2016). Aging-related renal injury and inflammation are associated with downregulation of Klotho and induction of RIG-I/NF-kappa B signaling pathway in senescence-accelerated mice. Aging Clin. Exp. Res. *28*, 69–76.

24. Allen, I.C., Moore, C.B., Schneider, M., Lei, Y., Davis, B.K., Scull, M.A., Gris, D., Roney, K.E., Zimmermann, A.G., Bowzard, J.B., et al. (2011). NLRX1 protein attenuates inflammatory responses to infection by interfering with the RIG-I-MAVS and TRAF6-NF-κb signaling pathways. Immunity *34*, 854–865.

25. Yevshin, I., Sharipov, R., Kolmykov, S., Kondrakhin, Y., Kolpakov, F., Kolpakov, and Fedor. (2019). GTRD: a database on gene transcription regulation—2019 update. Nucleic Acids Res. *47*, D100–D105.

26. Mathelier, A., Fornes, O., Arenillas, D.J., Chen, C.Y., Denay, G., Lee, J., Shi, W., Shyr, C., Tan, G., Worsley-Hunt, R., et al. (2016). Jaspar 2016: a major expansion and update of the open-access database of transcription factor binding profiles. Nucleic Acids Res. *44*, D110–D115.

27. Marx, C., Held, J.M., Gibson, B.W., and Benz, C.C. (2010). ErbB2 trafficking and degradation associated with K48 and K63 polyubiquitination. Cancer Res. *70*, 3709–3717.

28. Okamoto, M., Kouwaki, T., Fukushima, Y., and Oshiumi, H. (2017). Regulation of RIG-I activation by K63-linked polyubiquitination. Front. Immunol. *8*, 1942.

29. Bryan, K., Oralia, K., Krishanu, M., Reema, K., Chandra, E., and Bryan, K. (2015). Functional differentiation of ancestral RIG-I CARD1 and CARD2 domains occurred after the proliferation of RLR-IPS1 CARDs in deuterostomes, Due to Coevolution between RIG-I and IPS1 CARDs.

30. Zeng, Y., Wang, P.H., Zhang, M., and Du, J.R. (2016). Aging-related renal injury and inflammation are associated with downregulation of Klotho and induction of RIG-I/NF-κB signaling pathway in senescence-accelerated mice. Aging Clin. Exp. Res. *28*, 69–76.

31. Zhou, H.J., Li, H., Shi, M.Q., Mao, X.N., Liu, D.L., Chang, Y.R., Gan, Y.M., Kuang, X., and Du, J.R. (2017). Protective effect of klotho against ischemic brain injury is associated with inhibition of RIG-I/NF-κB signaling. Front. Pharmacol. *8*, 950.

32. Fumiaki, Ohtake, Y., Saeki, S., Ishido, Jun, K., Keiji, and Tanaka. (2016). The K48-K63 branched ubiquitin chain regulates NF-κB signaling. Mol. Cell. *64*, 251–266.

33. Fei, X., He, Y., Chen, J., Man, W., Chen, C., Sun, K., Ding, B., Wang, C., and Xu, R. (2019). The role of Toll-like receptor 4 in apoptosis of brain tissue after induction of intracerebral hemorrhage. J. Neuroinflammation *16*, 234.